Journal of Alloys and Compounds 776 (2019) 202–206

Contents lists available at ScienceDirect

Journal of Alloys and Compounds

journal homepage: http://www.elsevier.com/locate/jalcom

Denary high entropy metallic glass with large magnetocaloric effect

Juntao Huo [a, b, *], Jun-Qiang Wang [a, b, **], Wei-Hua Wang [c]

[a] CAS Key Laboratory of Magnetic Materials and Devices, Ningbo Institute of Materials Technology & Engineering, Chinese Academy of Sciences, Ningbo, Zhejiang 315201, China
[b] Zhejiang Province Key Laboratory of Magnetic Materials and Application Technology, Ningbo Institute of Materials Technology & Engineering, Chinese Academy of Sciences, Ningbo, Zhejiang 315201, China
[c] Institute of Physics, Chinese Academy of Sciences, Beijing, 100190, China

ARTICLE INFO

Article history:
Received 20 September 2018
Received in revised form
24 October 2018
Accepted 25 October 2018
Available online 26 October 2018

Keywords:
High-entropy alloys
Metallic glasses
Magnetocaloric effect
Magnetic entropy
Configurational entropy

ABSTRACT

We report the formation of a $Gd_{10}Tb_{10}Dy_{10}Ho_{10}Er_{10}Y_{10}Ni_{10}Co_{10}Ag_{10}Al_{10}$ denary high entropy metallic glass (HEMG). The magnetocaloric effect studies show that the denary HEMG possess large magnetic entropy changes over a wide temperature range, and thus a large refrigerant capacity. Combined with the simple alloy design of high entropy alloys and atomic level homogeneous single phase nature of metallic glasses, the magnetocaloric properties of HEMGs can be easily adjusted by changing the elements or configurational entropy. Our works show that the HEMG is a promising candidate material as the magnetic refrigerant.

Magnetic refrigeration has advantages of both high efficiency and environmental friendliness compared with conventional gas refrigeration, demonstrating their promising future [1–4]. The exploration of magnetic refrigerants with appropriate magnetocaloric effect (MCE) is the most important issue for practical applications, e.g. wide phase change temperature range and large refrigerant capacity. Over the past few decades, a large number of magnetocaloric materials have been developed [1–14], among which the rare earth (RE) based metallic glasses (MGs) have caused wide interests recently [7–14]. Compared to the crystalline alloys, RE-based MGs manifest large MCE over a much wider temperature range, higher electrical resistivity and thus smaller eddy current heating, high corrosion resistance, and outstanding mechanical properties, owing to their intrinsic amorphous nature and special compositions, which makes them suitable candidates for magnetic refrigerants [7].

Recently, combination of high-entropy alloys (HEAs) and MGs, a series of high-entropy metallic glasses (HEMGs) have been developed, which broke through the design concept of the conventional metallic glasses with one or two major elements [15–17]. The HEMGs with strong topological and chemical disorder have some unique or remarkably improved properties compared with the normal MGs or HEAs. Significantly, some HEMGs have been certified to possess distinctive magnetocaloric properties compared to RE-based MGs [18,19]. However, as one kind of special HEAs, there are some additional problems required to be investigated. For HEAs, the configurational entropy (ΔS_{config}), calculated as a function of alloy composition and the number of constituent elements (N), can be expressed as $\Delta S_{config} = R\ln N$. The equi-atomic composition in an alloy gives the greatest value of ΔS_{config}, which increases with increasing N via a formula with a logarithmic function [20]. However, how the ΔS_{config} affects the MCE of HEMGs is still indistinct. In addition, it is well known that HEAs possess four core effects: (1) Thermodynamics: high-entropy effects; (2) Kinetics: sluggish diffusion; (3) Structures: severe lattice distortion; and (4) Properties: cocktail effects [21]. One of the problems is if these effects still exist in high entropy metallic glasses.

In this paper, a novel HEMG with ten equal elements ($\Delta S_{config} = 2.3R$) i.e. $Gd_{10}Tb_{10}Dy_{10}Ho_{10}Er_{10}Y_{10}Ni_{10}Co_{10}Ag_{10}Al_{10}$ was fabricated. Its thermal, magnetocaloric properties have been studied.

* Corresponding author. CAS Key Laboratory of Magnetic Materials and Devices, Ningbo Institute of Materials Technology & Engineering, Chinese Academy of Sciences, Ningbo, Zhejiang 315201, China.
** Corresponding author. CAS Key Laboratory of Magnetic Materials and Devices, Ningbo Institute of Materials Technology & Engineering, Chinese Academy of Sciences, Ningbo, Zhejiang 315201, China.
E-mail addresses: huojuntao@nimte.ac.cn (J. Huo), jqwang@nimte.ac.cn (J.-Q. Wang).

https://doi.org/10.1016/j.jallcom.2018.10.328
0925-8388/

Compared to other materials, this HEMG exhibits excellent magnetocaloric effect.

The ingots with nominal compositions of $Gd_{10}Tb_{10}Dy_{10}Ho_{10}Er_{10}Y_{10}Ni_{10}Co_{10}Ag_{10}Al_{10}$ were prepared by arc melting pure Gd, Tb, Dy, Ho, Er, Y, Co, Ni, Ag and Al in a Ti-gettered argon atmosphere. Then the ingots were remelted and injected onto a spinning Cu roller to get the HE-MG ribbons. The amorphous nature of the samples was ascertained by X-ray diffraction (XRD) using a MAC Mo3 XHF diffractometer with Cu Kα radiation. Thermal analysis was carried out in a Perkin-Elmer DSC-7 differential scanning calorimeter (DSC). The temperature and field dependences of the magnetization were measured using a SQUID magnetometer (MPMS, Quantum Design). The heat capacity was measured using a physical properties measurement system (PPMS 6000, Quantum Design).

Fig. 1 shows XRD pattern (Fig. 1 a) and DSC traces (Fig. 1 b) of the as-cast $Gd_{10}Tb_{10}Dy_{10}Ho_{10}Er_{10}Y_{10}Ni_{10}Co_{10}Ag_{10}Al_{10}$ high entropy metallic glass ribbon. The XRD patterns show broad diffraction maxima, indicating the fully amorphous microstructure of the samples. From the DSC trace, it can be seen that an endothermic glass transition phenomenon occurs followed by several exothermic crystallization peaks, certifying the formation of glassy alloys. The glass transition temperature (T_g), first crystallization temperature (T_{x1}) and supercooled liquid region ($\Delta T_x = T_{x1}$-T_g) at the heating rate of 20 K/min are listed in Table 1. Similar to other HEMGs [18,19], the ΔT_x of the alloy, which is one of the important parameters in evaluating glass forming ability (GFA), are smaller than that of the other rare earth based MGs shown in Table 1, indicating their limited GFA. This may be attributed to the fact that the best GFA is usually found at or near the eutectic compositions, but the compositions of the denary HEMG alloy is far from the eutectic point, despite its high mixing entropy [19]. Surprisingly, although there are as many as ten elements, the denary HEMG can form a single amorphous phase, implying high-entropy effect also exists in the HEMGs. This is not to say that all multi-components in equal molar ratio can form a single amorphous phase at a high cooling rate. In fact, only carefully chosen compositions that satisfy the HEMG formation criteria will form a single amorphous phase instead of complicated crystalline phases. All these characteristics of HEMG are very similar to HEAs.

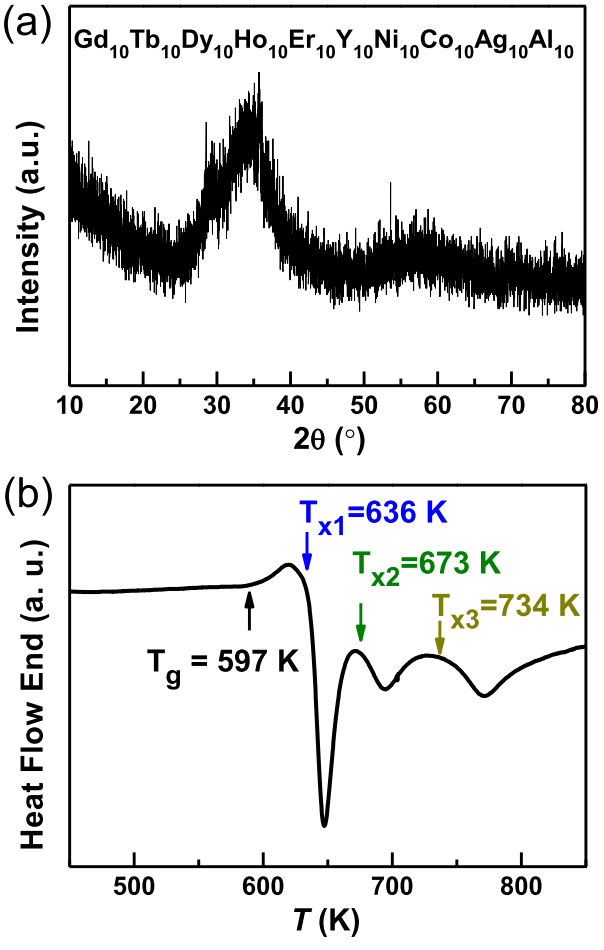

Fig. 1. (a) XRD pattern and (b) DSC trace of the as-cast denary high entropy metallic glass $Gd_{10}Tb_{10}Dy_{10}Ho_{10}Er_{10}Y_{10}Ni_{10}Co_{10}Ag_{10}Al_{10}$ ribbon.

To investigate the magnetic transition behavior of the denary HEMG, the temperature dependence of the magnetization (M-T) has been measured, as presented in Fig. 2. The curves were measured upon heating under a field of 200 Oe. The zero field cooling (ZFC) curve was cooled in zero field, and the field cooling (FC) curve was cooled in 200 Oe. In the FC curve, a spin freezing transition can be observed, while in the ZFC a cusp is observed at about 15 K where a divergence appears between the FC and ZFC branches, which is a typical spin-glass-like behavior [22]. The magnetic transition temperature (T_C) calculated from the differentiation of FC curve is 24 K, marked by arrows in the insert of Fig. 2.

The magnetic entropy change (ΔS_M) is usually used to characterize the magnetocaloric effect of the materials. In an isothermal magnetization process, the total ΔS_M of the system caused by the external magnetic field can be derived by integrating the Maxwell relation over the magnetic field [19]:

$$\Delta S_{\mathrm{M}}(T,H) = \int_{H\mathrm{min}}^{H\mathrm{max}} \left(\frac{\partial M}{\partial T}\right)_H dH, \tag{1}$$

where H_{min} and H_{max} represent the initial and final values of magnetic field, respectively. In this work, $H_{\mathrm{min}} = 0$ and $H_{\mathrm{max}} = 5$ T. To derive the temperature dependence of ΔS_M, the numerical approximation of the integral for Eq. (1) is applied in this work as following:

$$\Delta S_M(T,H) = \frac{\int_0^H M(T_i,H)dH - \int_0^H M(T_{i+1},H)dH}{T_i - T_{i+1}}. \tag{2}$$

By measuring the isothermal M-H curves at various temperatures T_i, as shown in Fig. 3 (a), the ΔS_M associated with the H variation can be evaluated according to Eq. (2). Fig. 3 (b) displays the ΔS_{M} as the function of the temperature and applied magnetic field for HEMG. Obviously, the magnetic entropy change decreases with decreasing field, but the shape of the curves remains approximately the same. The magnetic entropy change peak value $\left|\Delta S_M^{\mathrm{pk}}\right|$ under applied fields of 1–5 T are respectively 2.62 $\mathrm{Jkg^{-1}K^{-1}}$, 4.97 $\mathrm{Jkg^{-1}K^{-1}}$, 6.91 $\mathrm{Jkg^{-1}K^{-1}}$, 8.97 $\mathrm{Jkg^{-1}K^{-1}}$, and 10.64 $\mathrm{Jkg^{-1}K^{-1}}$, which are all near T_C and comparable to that of the most rare earth based MGs as listed in Table 1. In addition, the adiabatic temperature change (ΔT) under a magnetic field variation can be determined indirectly from the measured magnetization and the temperature dependence of heat capacity without magnetic field $C_0(T)$: $\Delta T(T, H) = T/C_0(T)^*\Delta S_{\mathrm{M}}(T, H)$ [23]. By this method the ΔT of denary HEMG under field changes of 1T, 2 T, 3 T, 4 T and 5 T is shown in Fig. 3 (c), the inset of which shows the temperature dependence of heat capacity under 0 T. The maximum values of ΔT are determined to be 6.66 K, 5.61 K, 4.32 K, 3.11 K and 1.64 K under

Table 1
The glass transition temperature T_g, first crystallization temperature T_x, supercooled liquid region ΔT_x, and magnetic transition temperature T_C (or peak temperature T_p), peak value of magnetic entropy change $|\Delta S_M^{pk}|$, refrigerant capacity RC under a maximum applied field of 5 T for present denary high entropy metallic glass. Data for the recently developed RE-based MGs and HEMGs are given for comparison.

NO.	Composition	T_g (K)	T_x (K)	ΔT (K)	T_p (K)	$\lvert\Delta S_M^{pk}\rvert$ ($Jkg^{-1}K^{-1}$)	δT_{FWHM} (K)	RC (Jkg^{-1})	Ref.
1	$Gd_{53}Al_{24}Co_{20}Zr_3$	606	672	66	93	9.4	83	780	[9]
2	$Gd_{55}Ni_{15}Al_{30}$	602	658	56	70	6.12	99	606	[10]
3	$Tb_{62.5}Co_{37.5}$	536	587	51	92.5	9.3	64	595	[11]
4	$Dy_{36}Ho_{20}Co_{20}Al_{24}$	633	687	54	23	9.49	44	417	[12]
5	$Ho_{36}Dy_{20}Al_{24}Co_{20}$	553	629	76	17	11.77	38	447	[13]
6	$Er_{50}Co_{20}Al_{24}Y_6$	651	702	51	8	15.91	26	423	[14]
7	$Gd_{20}Ho_{20}Er_{20}Co_{20}Al_{20}$	612	652	40	37	11.2	56	627	[18]
8	$Dy_{20}Ho_{20}Er_{20}Co_{20}Al_{20}$	632	668	36	18	12.6	37	468	[18]
9	$Gd_{20}Tb_{20}Dy_{20}Co_{20}Al_{20}$	594	626	32	58	9.43	67	632	[19]
10	$Gd_{20}Tb_{20}Dy_{20}Ni_{20}Al_{20}$	582	607	25	45	7.25	70	507	[19]
HE -MG	$Gd_{10}Tb_{10}Dy_{10}Ho_{10}Er_{10}$ -$Y_{10}Ni_{10}Co_{10}Ag_{10}Al_{10}$	597	636	39	29	10.64	50	532	This work

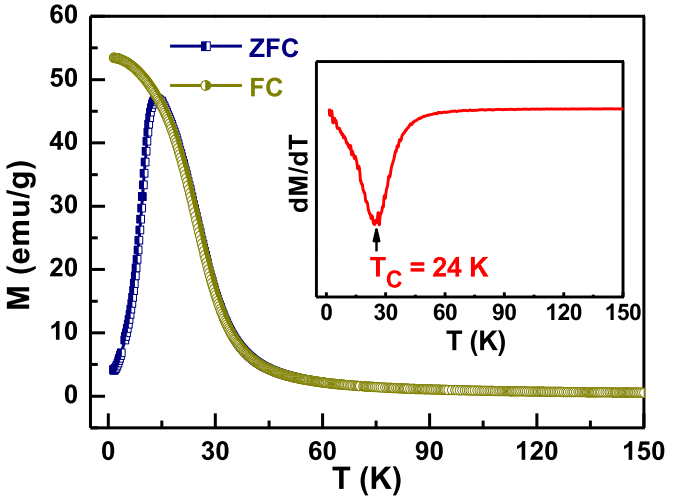

Fig. 2. Temperature dependence of the zero field cooling (ZFC) and field cooling (FC) magnetization under a magnetic field of 200 Oe for the denary HEMG. The inset presents the *dM/dT* versus temperature curves.

field changes of 5 T, 4 T, 3 T, 2 T and 1 T, respectively. These values are almost twice as large as Gd-based MG reported in reference 23.

The refrigerant capacity (RC) is another key parameter to characterize the efficiency of magnetic refrigerant, which is proportional to the area under the ΔS_M versus T curve. The RC in this work was estimated by taking the direct product of the maximum entropy change and the full width at half-maximum of the peak (δT_{FWHM}) [24], RC $= |\Delta S_M^{pk}| \times \delta T_{FWHM}$. The RC value for the denary HEMG is determined to be 532 Jkg^{-1}. This value is much larger than that of the $Gd_5Si_2Ge_2$ (305 Jkg^{-1}) [3] and $Gd_5Si_2Ge_{1.9}Fe_{0.1}$ (360 Jkg^{-1}) [4], indicating the better refrigerant efficiency of the HEMG. The high RC should be attributed to the large ΔS_M and the particular glassy structure which extends the large ΔS_M to a wider temperature range, which could be ascribed to the combination of the spin glass behavior and complicated compositions in this HEMG. In spin-glass phase, moments are frozen into equilibrium orientations, but there is no long-range order [25], which makes it more difficult to be frozen than the ferromagnetic materials. Therefore, the spin glass and complicated compositions of the HEMG can widen the magnetic transition temperature range, which will broaden the ΔS_M peaks and thus increase the value of RC. The large magnetic entropy change and excellent refrigerant capacity, combining the intrinsic nature of MGs, may promote the practical applications of the HEMG as a kind of magnetic refrigerant.

Furthermore, the magnetic field dependences of maximum magnetic entropy change and refrigerant capacity for the denary HEMG are investigated. As shown in Fig. 4, the ΔS_M^{pk} and RC can be expressed as $\Delta S_M^{pk} \propto H^n$, and RC $\propto H^N$, respectively [26]. The exponents n and N, controlled by the critical exponents of the alloy series, can be extracted through fitting the experimental data in Fig. 4 with the relations. For the HEMG alloy, $n = 0.87 \pm 0.01$, and $N = 1.17 \pm 0.01$, both are about equal to that of other HEMGs [18,19]. The exponents n near the transition temperature for HEMGs deviate from the predicted value (~2/3) near the transition temperature, probably owing to the failure of the mean field picture in the critical region [27].

Cocktail effect is usually used to describe the phenomenon that the unexpected properties of metallic alloys can be obtained after mixing many elements, which has been subsequently confirmed in the mechanical and physical properties [28–31]. The cocktail effect in magnetocaloric properties is firstly investigated for high entropy metallic glass. Fig. 5 shows the comparison of the $|\Delta S_M^{pk}|$, RC and peak temperature (T_P, near the magnetic transition temperature) for the present HEMG and the other metallic glasses listed in Table 1. Obviously, it can seen that the $|\Delta S_M^{pk}|$, RC and T_P of the denary HEMG are different from that of rare earth (Gd, Tb, Dy, Ho, Er) based metallic glasses and reported HEMGs with five equal elements ($\Delta S_{conf} = 1.6R$). It means that the magnetocaloric properties can be easily adjusted by the composition change, changing the elements or the configurational entropy. However, the magnetocaloric properties of denary HEMG are not unexpected, which means there is not distinct cocktail effect in magnetocloric HEMGs. HEMG design is the simplest among those for metallic materials. Specifically, as few as two factors, element number N and equiatomicity, are required in alloy design. Due to the absence of crystalline phase, metallic glasses can be considered to be atomic level homogeneous single phase. Therefore, according to the required magnetocaloric properties (including the $|\Delta S_M^{pk}|$, ΔT, RC and T_P), one can chose elements of different types and quantities to prepare high entropy metallic glasses used as magnetic refrigerants.

In summary, the large magnetic entropy change and excellent refrigerant capacity have been obtained in $Gd_{10}Tb_{10}Dy_{10}Ho_{10}Er_{10}$-$Y_{10}Ni_{10}Co_{10}Ag_{10}Al_{10}$ high entropy metallic glass. The magnetic transition of the HRMG shows a spin glass behavior. The spin glass transition and large configurational entropy ($\Delta S_{config} = 2.3R$) make the HEMG possess a large magnetocaloric effect over a much wider temperature range. Its $|\Delta S_M^{pk}|$, ΔT and RC under an applied field of

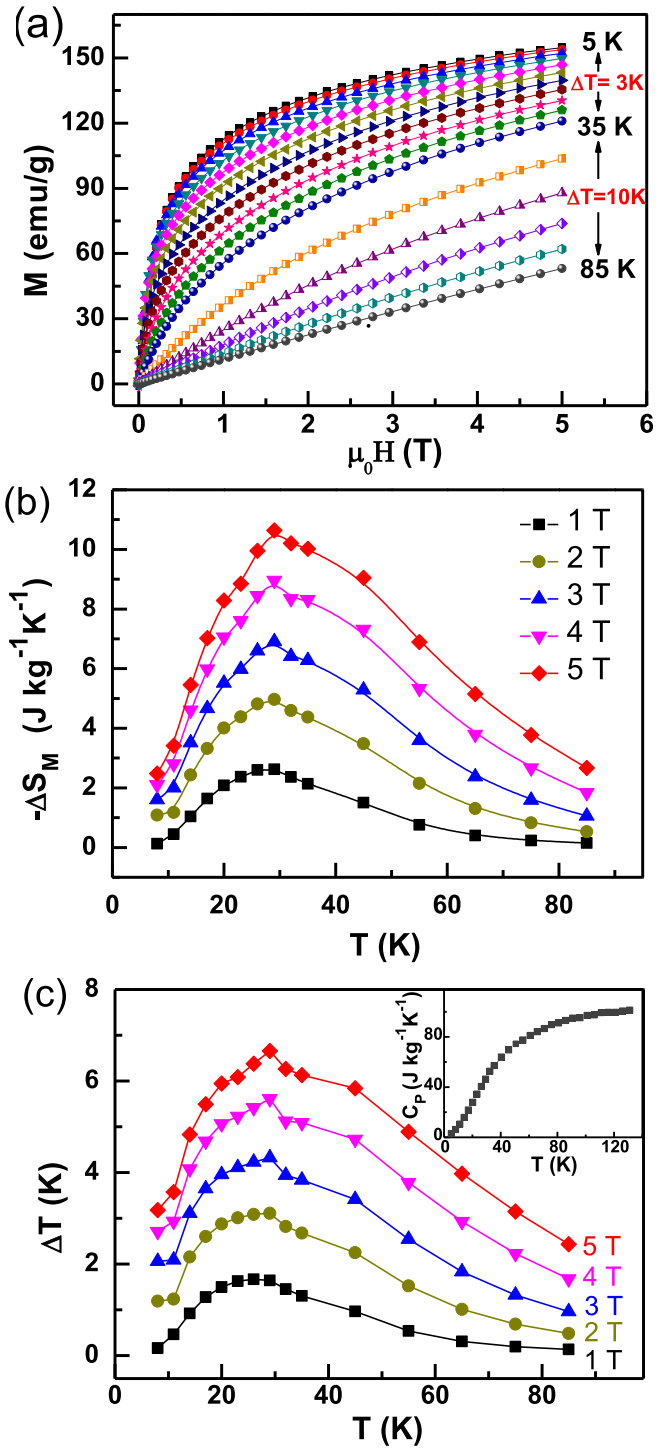

Fig. 3. (a) Isothermal magnetization curves, (b) Magnetic entropy changes and (c) Adiabatic temperature changes as a function of temperature under a maximum applied field of 1 T, 2 T, 3 T, 4T and 5 T for the denary HEMG measured at temperatures between 5 and 85 K. Temperature intervals of 3 K and 10 K were selected for the regions 5–35 K and 35–85 K, respectively. The inset shows the temperature dependence of heat capacity under 0 T.

5 T can reach 10.64 $Jkg^{-1}K^{-1}$, 6.66 K and 532 Jkg^{-1}, respectively, which are comparable to rare earth based MGs. Combined with the simple alloy design of HEAs and atomic level homogeneous single phase nature of MGs, the $|\Delta S_M^{pk}|$, ΔT, RC and T_P of HEMG can be easily adjusted by changing the elements or configurational

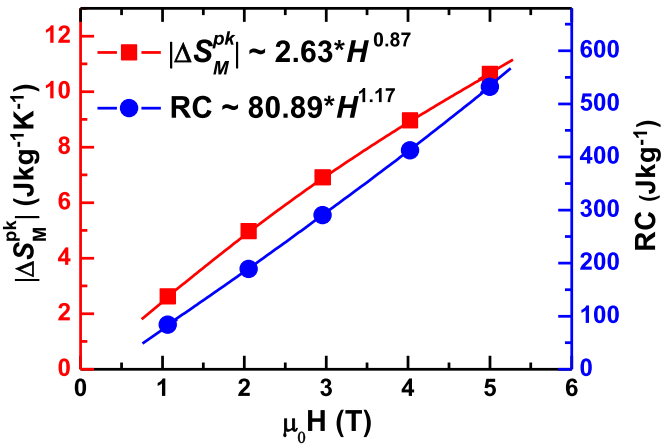

Fig. 4. Magnetic field dependence of the maximum magnetic entropy change ($|\Delta S_M^{pk}|$, red line), and refrigerant capacity (RC, blue line) for the denary HEMG. The solid curves are fitting results of $|\Delta S_M^{pk}| \propto aH^n$ and $RC \propto AH^N$, respectively. (For interpretation of the references to colour in this figure legend, the reader is referred to the Web version of this article.)

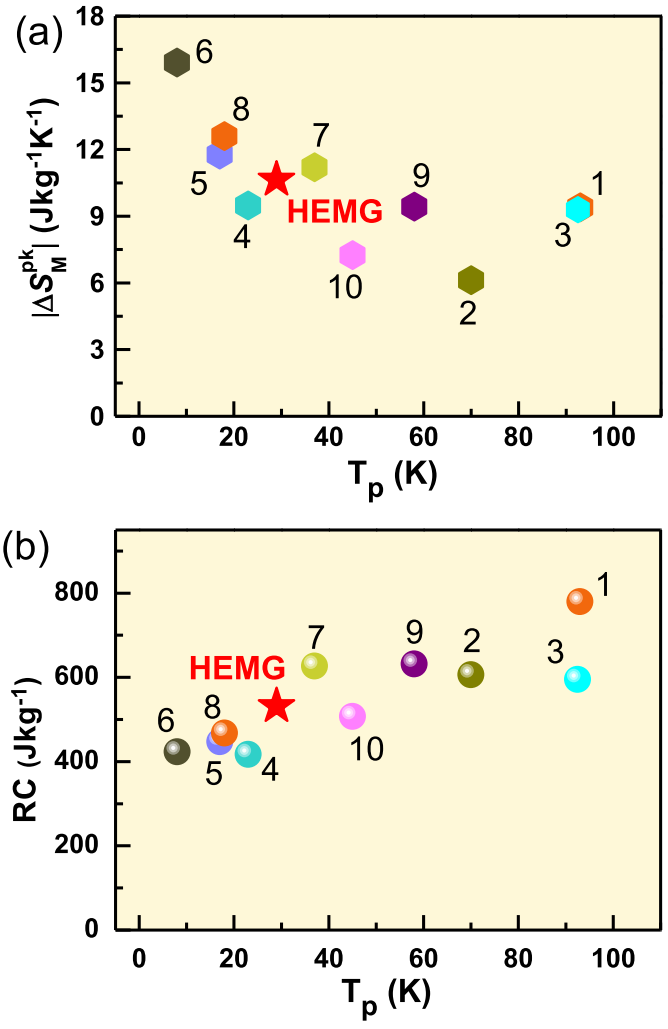

Fig. 5. The compositions of (a) maximum magnetic entropy change ($|\Delta S_M^{pk}|$), and (b) refrigerant capacity (RC) for the denary HEMG and other metallic glasses listed in Table 1.

entropy. All of the above characteristics make the HEMG a promising candidate as magnetic refrigerants.

Acknowledgements

This work was supported by the National Natural Science Foundation of China (Grant No. 51771217, 51771216), Zhejiang Provincial Natural Science Foundation of China (Grant No. LY17E010005) are acknowledged.

References

[1] A. Smith, K.K. Nielsen, C.R.H. Bahl, Phys. Rev. B 90 (2014), 104422.
[2] Y. Yuan, Y. Wu, X. Tong, H. Zhang, H. Wang, X.J. Liu, L. Ma, H.L. Suo, Z.P. Lu, Acta Mater. 125 (2017) 481–489.
[3] V.K. Pecharsky, K.A. Gschneidner Jr., Phys. Rev. Lett. 78 (1997) 4494–4497.
[4] V. Provenzano, A.J. Shapiro, R.D. Shull, Nature 429 (2004) 853–857.
[5] F.X. Hu, B.G. Shen, J.R. Sun, G.J. Wang, Z.H. Cheng, Appl. Phys. Lett. 80 (2002) 826–830.
[6] J. Liu, T. Gottschall, K.P. Skokov, J.D. Moore, O. Gutfleisch, Nat. Mater. 11 (2012) 620–626.
[7] Q. Luo, W.H. Wang, J. Alloys Compd. (495) (2010) 209–216.
[8] J.T. Huo, D.Q. Zhao, H.Y. Bai, E. Axinte, W.H. Wang, J. Non-Cryst. Solids 359 (2013) 1–4.
[9] Q. Luo, D.Q. Zhao, M.X. Pan, W.H. Wang, Appl. Phys. Lett. 89 (2006), 081914.
[10] F. Yuan, J. Du, B.L. Shen, Appl. Phys. Lett. 101 (2012), 032405.
[11] B.Z. Tang, D.Q. Guo, L. Xia, D. Ding, K.C. Chan, J. Alloys Compd. 728 (2017) 747–751.
[12] L. Liang, X. Hui, C.M. Zhang, G.L. Chen, J. Alloys Compd. 463 (2008) 30–33.
[13] L. Liang, X. Hui, C.M. Zhang, Z.P. Lu, G.L. Chen, Solid State Commun. 146 (2008) 49–52.
[14] Q. Luo, D.Q. Zhao, M.X. Pan, W.H. Wang, Appl. Phys. Lett. 90 (2007), 211903.
[15] K. Zhao, X.X. Xia, H.Y. Bai, D.Q. Zhao, W.H. Wang, Appl. Phys. Lett. 98 (2011), 141913.
[16] H.F. Li, X.H. Xie, K. Zhao, Y.B. Wang, Y.F. Zheng, W.H. Wang, L. Qin, Acta Biomater. 9 (2013) 8561–8573.
[17] H.Y. Ding, K.F. Yao, J. Non-Cryst. Solids 364 (2013) 9–12.
[18] J.T. Huo, L.S. Huo, J.W. Li, H. Men, X.M. Wang, A. Inoue, C.T. Chang, J.Q. Wang, R.W. Li, J. Appl. Phys. 117 (2015), 073902.
[19] J.T. Huo, L.S. Huo, H. Men, X.M. Wang, A. Inoue, J.Q. Wang, C.T. Chang, R.W. Li, Intermetallics 58 (2015) 31–35.
[20] J.W. Yeh, S.K. Chen, S.J. Lin, J.Y. Gan, T.S. Chin, T.T. Shun, C.H. Tsau, S.Y. Chang, Adv. Eng. Mater. 6 (2004) 299–303.
[21] Y. Zhang, T.T. Zuo, Z. Tang, M.C. Gao, K.A. Dahmen, P.K. Liaw, Z.P. Lu, Prog. Mater. Sci. 61 (2014) 1–93.
[22] J.T. Huo, Q. Luo, J.Q. Wang, W. Xu, X.M. Wang, R.W. Li, H.B. Yu, AIP Adv. 7 (2017), 125014.
[23] Q. Luo, J. Shen, Intermetallics 92 (2018) 79–83.
[24] K.A. Gschneidner, V.K. Pecharsky, A.O. Pecharsky, C.B. Zimm, Mater. Sci. Forum 69 (1999) 315–317.
[25] S. David, K. Scott, Phys. Rev. Lett. 35 (1975) 1792–1795.
[26] J.Y. He, W.H. Liu, H. Wang, Y. Wu, X.J. Liu, T.G. Nieh, Z.P. Lu, Acta Mater. 62 (2014) 105–113.
[27] Q. Luo, B. Schwarz, N. Mattern, J. Shen, J. Eckert, AIP Adv. 3 (2013), 032134.
[28] Y.J. Zhou, Y. Zhang, Y.L. Wang, G.L. Chen, Appl. Phys. Lett. 90 (2007), 181904.
[29] X.F. Wang, Y. Zhang, Y. Qiao, G.L. Chen, Intermetallics 15 (2007) 357–362.
[30] S. Singh, N. Wanderka, B.S. Murty, U. Glatzel, J. Banhart, Acta Mater. 59 (2011) 182–190.
[31] C. Li, J.C. Li, M. Zhao, Q. Jiang, J. Alloys Compd. 475 (2009) 752–757.